Application of Microcontroller ATmega8535 for Hybrid Photovoltaic – Thermal (PV/T)

Syafaruddin [1], Andani Achmad [2], Tajuddin Waris [3], Zulkifli Tahir [4], Yulianto Dwi Putra [5]

Department of Electrical Engineering of Universitas Hasanuddin, 90245 Tamalanrea-Makassar, Indonesia
[1] syafaruddin@unhas.ac.id
[2] andani.achmad@icloud.com
[3] tajuddinwaris24@yahoo.com
[4] zulkifli@unhas.ac.id
[5] yuliantodwiputra@yahoo.co.id

***Abstract*—It is well-known that the electrical efficiency conversion of photovoltaic systems is low due to non-linear semiconductor mechanism inside the solar cell materials. The increasing in output efficiency will be always very challenging to photovoltaic technology. One of the methods is to utilize the thermal energy arises in the back side of module, which may be called hybrid photovoltaic-thermal (PV/T). The advantage of this system is the output of electricity and thermal energy can be obtained simultaneously. In addition, the electrical efficiency can be indirectly improved since the thermal system acts as cooling system. In this research, thermal energy extraction mechanism is based on the performance of microcontroller ATmega8535 including thermal sensors. The idea is the microcontroller will operate pump to flow the media fluid through designed spiral pipe once the threshold temperature inside the heat box extraction is reached, therefore high temperature fluid can be observed in the outlet pipe. Several testing on three different fluids, air, water and thermal oil under clear sky, cloudy sky and rainy conditions are conducted in order to confirm the proper working condition of control system.**

Keywords: hybrid photovoltaic-thermal, microcontroller ATmega8535, thermal sensor, control circuit, fluid media.

I. INTRODUCTION

Countries which are located in the equator region are blessed with high potential of solar energy. It is due to the small change of incident angle of sunlight direction that makes the irradiance level can be constantly maintained at high level for years. According to the NASA measurement in Indonesia, the intensity of sunlight reaching the surface is about 5.5kWh/m^2 per-day. It means high power output of photovoltaic system can be expected for wide area installation systems. In facts, only very small portion of solar energy can be utilized as electrical and thermal energy. For the photovoltaic system utilization, we are still facing several problems such as complex manufacturing process and material technology limitation that lead to high cost module encapsulation and installation of photovoltaic systems. Another problem is the output power is fluctuated under irradiance level and cell temperature change. In some cases such as partial shading conditions, it is difficult to find the optimal operating point; unless deployment of very sophisticated control techniques that may lead to increase the overall cost installation systems. But, the most important technical point related to the photovoltaic system practice is the low efficiency compared to other types of power generation systems.

From the basic technical point of view, the low efficiency energy conversion is due to the semiconductor behavior of Silicon as the basic component of solar cell in responding the irradiance level. Even if the solar cell is considered ideal, the efficiency is not more than 40%. In fact, there will be absorption, reflection coefficients of solar cell material and other factors that influence to the electrical conversion mechanism. Therefore, in real practice of PV system, the solar cell with crystalline Silicon will have efficiency not more than 15% and about 10% for the solar cell with non-crystalline Silicon technology. The performance is highly affected by the temperature variations, especially for Silicon technology where the temperature increases, the voltage diffusion in p-n-junction reduces to make the open-circuit voltage change about -2.1 mV/K. Recently, the PV system technology developed for much higher efficiency to about 30-35% for CIGS technology but this is only for specific applications and also the cost is quite expensive compared to the mature Silicon technology.

Apart from material technology, the efficiency conversion of photovoltaic system can be increased by implementing the maximum tracking control technique. It is the way that whatever the input parameters change, the operational point can be maintained at the optimal output power. However, the sophisticated tracking control techniques still need further experimental works to reach the practical level of PV system due to they may come with additional electronic devices that need to be coordinated with the PV power conditioning systems. Therefore, it is going to be other ways to increase the PV system efficiency by utilizing the thermal energy

produced at the backside of the module. The high density of energy thermal can be observed at the back side of PV module is caused by resistivity material composing the PV module that is encapsulated by module frame and more intensify by the ambient temperature. The photovoltaic system with utilizing thermal energy is well-known as hybrid photovoltaic-thermal. At glance, the thermal system functions as radiator system, therefore the implementation of this system will make the electrical efficiency increases simultaneously due to the reduction of negative temperature-voltage coefficient effects.

Research and development of hybrid photovoltaic-thermal technology has been investigated since 1970 with significant improvement in innovation of manufacturing products [1]. The significant outputs are new theory come up with field testing including identification of several important parameters. The design and experimental thermal photovoltaic for the building exterior applications have been attracted much attention since the last decade. The development is focused on the thermal extraction method through air circulation between photovoltaic cell and thermal insulation of building exterior [2]. In this research, the simultaneous capability of power generation and thermal extraction during winter was the priority investigation. Some researchers are concentrated on the exergy analysis or the maximum capability of system to produce energy according to the thermodynamic process. The thermodynamic efficiency and exergy system efficiency have been recorded for region in India to about 55-65% and 12-15%, respectively; where these values are very close to the predicted efficiency performed by other researchers in Denmark [3]. For more detailed energy and exergy analysis with constant air quantity has been investigated for micro scale hybrid photovoltaic thermal under frame design and climate parameters in India [4]. The calculation results showed that the thermal energy and exergy level can be increased to about 70% and 60%, respectively.

The building integrated PV system approach is the most rational concept to increase the performance of photovoltaic systems. In fact, the BIPV system does not only improve the system efficiency regarding to electricity and thermal output simultaneously, rather to improve the thermal insulation of building structure [5]. The computer simulation was utilized to analyze the dependency between solar cell packages, velocity of fluid and electricity efficiency; the simulation results shown that there will be an optimal fluid flow to guarantee the high integration of performance in energy output. The research then continued to study the system sensitivity for water heating system with natural circulation using photovoltaic module of single crystalline Silicon [6]. The simulation and field experimental works were performed by considering several factors, such as air mass, solar cell packages and light transmission on the module absorber in order to obtain better performance of integrated PV-thermal system. Indeed, the computer simulation of hybrid photovoltaic system using Matlab/Simulink becomes more interesting to find the best strategic model for thermodynamic process that represents the hybrid photovoltaic-thermal system [7]. The simulation results revealed that computer Matlab/Simulink method is well enough to represent the overall hybrid PV systems by considering measurable code, fast time development and simply integrated with other computational techniques rather than implementing conventional language programming.

The improving efficiency of hybrid photovoltaic-thermal does make sense in terms of electrical and thermal efficiency. With proper design, the electrical efficiency can be further extended as results of ‘radiator system’ that provides cooling effect on PV module. In fact, the application of hybrid photovoltaic-thermal is not only for the heating demand system but for cooling system as well. Some study results indicate that integrated PV systems is potential to be the promising energy source for heating and cooling demand system for household applications in the future [8]. The overall performance can be improved further by combination with other thermal sources, such as combined heat and power (CHP). The technique is implemented to anticipate the temporal distribution of flux radiation of sunlight [9].

The technology of cell materials is also identified as the important factors for hybrid photovoltaic-thermal [10], [11]. The main purpose of hybrid photovoltaic-thermal is to provide cooling system that effects to the increase the electrical energy output, although sometimes other parts may respond under their standards. Therefore, the amorphous Silicon technology is commended for designing hybrid photovoltaic thermal due to the low *negative temperature coefficient* that means the increase in temperature will not effect to decreasing in output voltage. In addition, the temperature operation of amorphous Silicon is very high as one of the important requirement for the thermal system. The amorphous Silicon is recognized as the potential candidate for the development of hybrid solar thermal in the future. The evaluation in the energy matrix for the hybrid photovoltaic-thermal design system has been investigated based on the photovoltaic cell technology. Five PV module technologies such as c-Si, p-Si, a-Si (thin film), CdTe and CIGS have been considered according to the overall thermal energy analysis and potential exergy [12].

This research is focused on the improving mechanism of the fluid flow by implementing the microcontroller ATmega8535 as the pump driver to fluid media once sensor reaches the temperature threshold. For this reason, the back side of photovoltaic module is modified by encapsulating with thermal insulation material and setting piping system in the air cavity between the module and the wall insulation material. The idea is the microcontroller will operate pump to flow the media fluid through designed spiral pipe when the temperature

inside the air cavity increases, therefore high temperature fluid can be observed in the outlet pipe. Other supporting components are windshield wisher pumps, temperature sensor of LM35D2 and language programming of Code Vision AVR for the microcontroller utilization. Several testing on three different fluids, air, water and thermal oil is conducted in order to confirm the proper working condition of microcontroller. Further control development of hybrid photovoltaic-thermal in this research is oriented for the building integrated photovoltaic (BIPV) systems.

II. State of Art of Hybrid Photovoltaic-thermal (PV/T)

It is well-known that the photovoltaic systems conventionally produce electrical energy by direct conversion from sun energy. However, the electrical efficiency conversion is not so high because majority portion of sunlight energy on the module surface is reflected and transferred to thermal energy. The increasing in temperature significantly reduces the output power by means further reducing electrical efficiency conversion. Therefore, providing additional system to absorb the thermal effect at the back side of the PV module tends to improve the photovoltaic system performance. Consequently, additional output energy can be observed in the form of thermal energy, therefore improving the overall efficiency conversion of PV system.

The structure of hybrid photovoltaic-thermal to produce electric and thermal energy simultaneously is not a new thing but the control design is rapidly developed. The main structure is the piping system as the media flow of fluid installed in the bottom parts of module between air cavities under encapsulation of thermal insulation material. The fluid is intentionally flown by means of controlling system once the temperature increases to certain level. For this reason, it is important to design the control in order to guarantee that the thermal energy is successfully extracted. The configuration of control circuit based on the microcontroller ATmega8535 utilization for hybrid photovoltaic-thermal design is shown in Fig. 1.

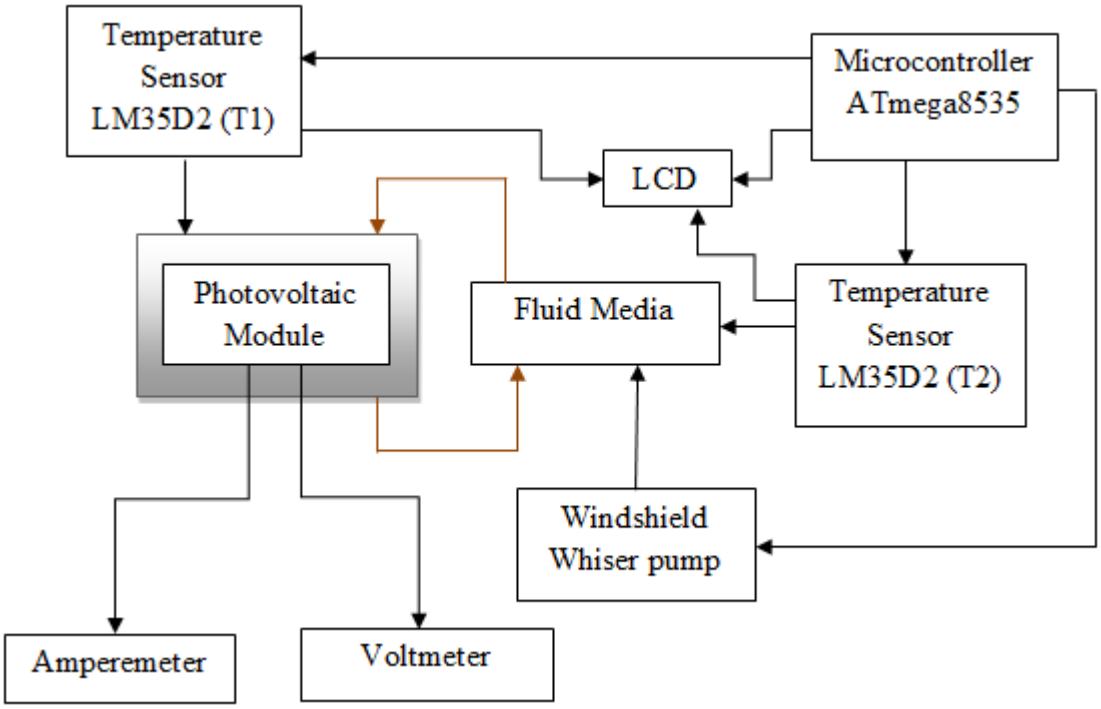

Fig. 1. Proposed control mechanism for hybrid photovoltaic-thermal

In the schematic configuration, the photovoltaic module is placed over designed box that functions as encapsulation for the thermal energy. The box for the heat has dimension of 85x55x10 cm^3 following the size area of photovoltaic module. The purpose to set 10 cm high for the box is to allow the spiral pipe not touching the any parts of module and box in order to narrowing the space of thermal extraction. Meanwhile, the copper spiral pipe is constructed with 17 indentations by 50 cm long which is according to wide of box extraction. Indentation is intentionally made to allow high fluid discharge. The copper pipe is spirally arranged inside the box as shown in Fig. 2 that functions as medium of fluid flow. The temperature sensor of LM35D2 (T1) is located inside the box to measure the temperature at back side of PV module. A windshield whiser pump is used to pump the fluid media through the spiraling pipe and fluid storage. Another temperature sensor LM35D2 (T2) is located inside the fluid storage to measure the fluid outlet temperature. Both temperature measurements are then displayed in liquid crystal display (LCD).

Fig. 1. Construction of spiral Copper pipe in the box extraction

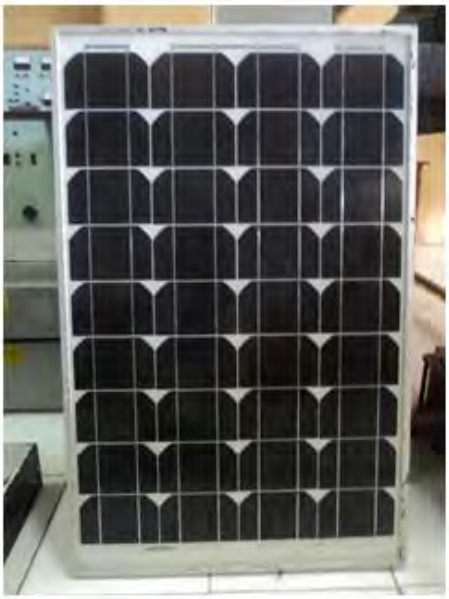

a. PV module

b. windshield whiser pump

Fig. 3. The physical appearance of photovoltaic module and windshield whiser pump

In addition, the control circuit which is mainly the microcontroller of ATmega8535 and other electronic components respond following the instruction by designed program written in C and compiled in Codevision AVR software. The algorithm is very simple which is only based on the temperature threshold set inside the encapsulated box. If this temperature reaches value higher than 45°C then microcontroller operates windshield whiser motor to pump the fluid through the spiraling pipe back to the fluid storage. The microcontroller circuit

also regulates sensor performance, motor pump and LCD monitor. In order to measure the electrical output power, the Voltmeter and Amperemeter are connected in the output terminal of PV module.

The physical appearance of photovoltaic module and windshield whiser pump is shown in Fig. 3. The type of photovoltaic module is multi crystalline Silicon of 50 Wp, while the windshield whiser pump is similar to the dc motor with IC L293D as pump driver controlled by microcontroller ATmega8535. The technical specification of PV module and windshield whiser pump is presented in Table I, while other supporting components for design of hybrid photovoltaic thermal is shown in Table II.

TABLE I
Technical specification of photovoltaic module and windshield whiser pump

PV Module		**Windshield Whiser Pump**	
Module Type	: WJ50-M (854 x 541 x 30) mm	Brand name	: INXT
Rate maximum power	: 50 Wp	Model number	: AWP107-10
Tolerance	: ± 5 %	Rated voltage	: 12/24 Volt
Open circuit voltage (V_{oc})	: 21.6 V	Weight	: 0.065KG
Short circuit current (I_{sc})	: 3.01 A	Color	: Black
Maximum power voltage (V_{mp})	: 17.6 V	Material	: PA6+30% GF, ABS
Maximum power current (I_{mp})	: 2.84 A	Flow Rate	: 2400ml/min
Working Temperature	: -45°C to +35°C	Certification	: ISO/TS 16949
Irradiance	: 1000 W/m^2		
Weight	: 5 kg		

Table II
Other supporting components for design of hybrid photovoltaic thermal

Components	**Qty**
Copper pipe 3/8”	13 m
Triplex box	1
Plastic pipe 5/8”	2.03 m
Resistor 4.7 Ω	1
Resistor 1 KΩ	3
Capacitor 22 pF	2
Capacitor 100 nF	3
Capacitor (elco) 1000 µF	1
Diode 2A	1
LED	1
Regulator 7805	2
LCD	1
L293D	1
LM35D2	2
Xtall	1
Rainbow cable	1.5 m

The control circuit is developed according to the AVR microcontroller utilization. In general, the architecture of AVR microcontroller has RISC 8 byte, where all instructions are packaged in 16 byte code and majority of instruction are executed in 1 cycle of clock. Therefore, the time execution for instruction is totally different with MSC51 microcontroller where it requires 12 cycle of clock. The AVR and MSC51 microcontrollers are totally

different in terms of architecture where AVR based on RISC (Reduced Instruction Set Computing) technology, while MCS51 based on CISC (Complex Instruction Set Computing) technology. In addition, the AVR microcontroller is divided into four classes of family, i.e ATtiny, AT90Sxx, ATmega and AT86RFxx. Their architecture are basically similar, they are mainly difference in memory, peripheral and function.

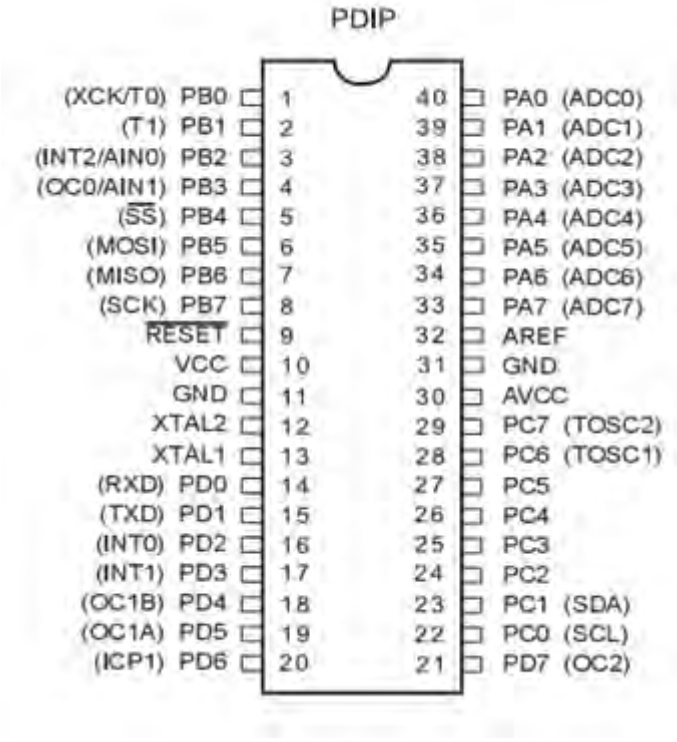

Fig. 4. Pin configuration of AVR microcontroller ATmega8535

In this research, the AVR microcontroller ATmega8535 is utilized. The pin configuration can be seen in Fig. 4. According to this figure, the microcontroller has some important features and capabilities for instance there are 32 of I/O port divided into Port A, Port B, Port C and Port D, 8 byte microprocessor system based on RSIC with maximal speed of 16 MHz; 8 channel of 10 byte internal ADC, 3 timer/counter with comparator capability, 32 registry of CPU, watchdog timer with internal oscillator, SRAM with 512 bytes, flash memory with 8 Kb with Real While Write capability. They also have internal and external unit interruption, SPI port interface, EEPROM with 512 byte that can be programmed during operation, analog comparator interface and USART port for serial communication with 2.5 MBps.

III. HARDWARE AND SOFTWARE DESIGN IN CONTROL CIRCUIT

Apart from the explanation related to design of box extraction and spiral arranged copper pipe which is not the main purpose of this research, the hardware and software design will be explained in this section. The complete connection in control circuit is shown in Fig. 5. For the control design of hybrid photovoltaic thermal based on the AVR microcontroller ATmega8535 utilization, all ports A, B and D are used. Port A (PA.0 and PA.3) are connected to thermal sensor of LM35D2, port B (PortB.0 to PortB.7, except portB.3) is connected to the input of LCD and port D (PD.2 and PD.4) are connected to the input of IC L293D for dc motor driver (windshield whiser pump). The motor driver (IN.1 to IN.4) is connected to the microcontroller through port PD.2, while other pins (EN.1 and EN.2) connected through port PD.4. In addition, RESET pin is connected to the XTAL1 and XTAL2 pins for external clock input to reset the microcontroller operation. Meanwhile the VCC pin is for the input dc voltage of 5 Volt.

Meanwhile, the software design is based on the media editor program and compiler using Code Vision AVR. The CodeVision AVR is one of the compiler software programs for the utilization of microcontroller AVR family. Probably, this software is the best amongst others according to the capability of using *Integrated Development Environment* (IDE) including the facility of editing program, compiling and downloading with interactive editor setting. Also, it has the capability of generating program code automatically with CodeWizardAVR. Other features are facility to download program directly from CodeVisionAVR using special hardware, such Atmel STK500, Canadian System of STK200+/300 and other hardware defined by CodeVisionAVR. In addition, it has debugger facility to accommodate other types of compiler, such as

AVRStudio and has serial communication terminal to check program that is specially made using UART serial communication facility.

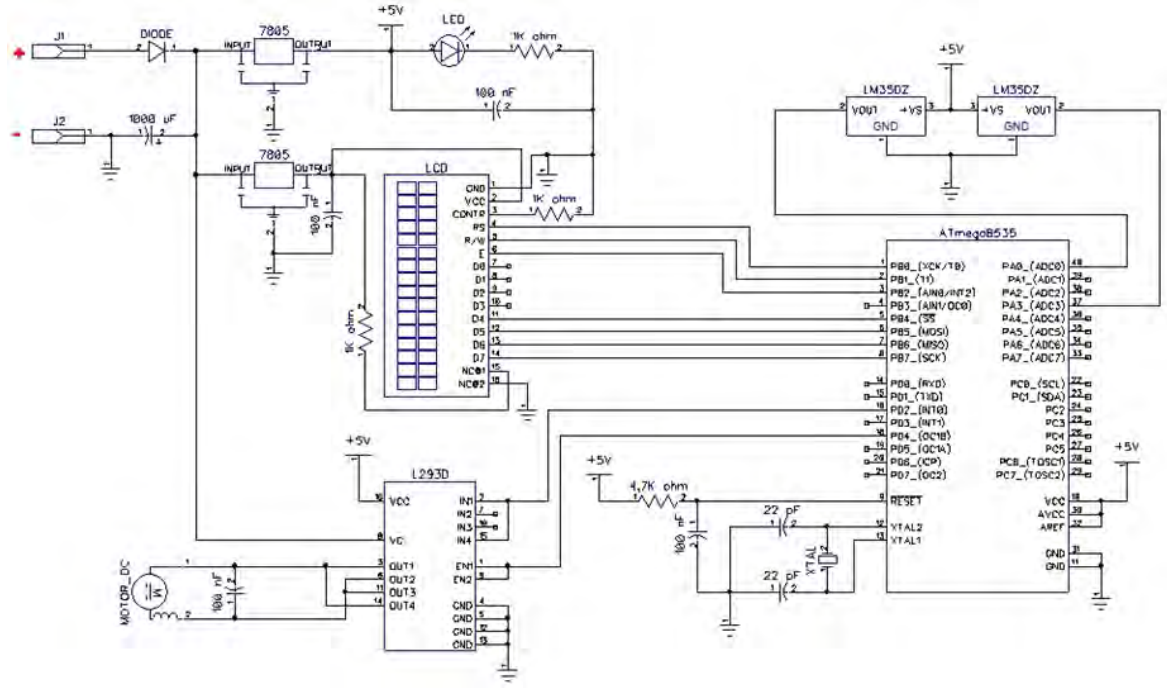

Fig. 5. Complete connection in control circuit

The program algorithm constructed in C language for microcontroller operation is developed as follows. The first step is to run the initialization I/O, LCD and LM35D2 in order to activate I/O ports of microcontroller. After initialization, the program will read the thermal sensor measurement LM35D2 (T1) located in the box extraction. The microcontroller will display this measurement in LCD including the thermal sensor measurement LM35D2 (T2) in the fluid storage, while the dc motor is still off. Once the temperature reaches 45^{o}C, the microcontroller sends signal to windshield whiser pump to pump fluid flowing to the spiral pipe in the box extraction. Otherwise, the pump remains off. The microcontroller is continually sending signal to ensure the motor driver operate under expected operation. The overall operation only can be terminated if the control circuit is deactivated by means turn-off the power supply.

IV. Design Results and Testing

In this experiment, the electrical parameters (voltage and current) and thermal parameter (temperature) are measured simultaneously using the experimental design system shown in Fig. 6. The control performance is tested for three different types of fluids, such as water, thermal oil and air under different weather conditions (clear sky, cloudy sky and rain). The data measurement is normally taken from 9 a.m to 2 p.m and the temperature threshold as the reference controller is 45°C.

In the electrical measurement, the photovoltaic module is connected to the Voltmeter and Amperemeter in order to measure the output power. The measured power is the output power after the control circuit which is actually composed of linear and non-linear load. The important consideration is the windshield whiser pump that acts as non-linear load. When the pump is activated, it will effect to the decrease in voltage and increase in current. However, the deviation of this value is still in the tolerable level; therefore the overall system functions. Meanwhile, only the temperature difference between the box extraction and fluid storage is considered in the thermal power measurement.

Fig. 6. Experimental design

The efficiency calculation is based on the ratio between output power and input power. The electrical efficiency (η_e) of PV module is about 10.69% following the calculation:

$$\eta_e = \frac{P_{output}(\max)}{P_{input}(\max)} x100\% \quad (1)$$

where P_{output}(max) is the maximum available output power for PV module (50 W) and P_{input}(max) is multiplication between the maximum global irradiance (1000 W/m^2) and surface area of PV module (0.4675 m^2); therefore P_{input}(max)= 467.5 W. Nevertheless, the electrical power output measurement is simply calculated as:

$$P_{out1} = VxI \quad (2)$$

where V and I are the voltage and current measurements, respectively.

For the thermal efficiency calculation, the heat energy of fluid is determined by:

$$\Delta Q = mc(T_2 - T_1) \quad (3)$$

where the mass (m) of water, thermal oil and air are 15 kg, 1.8 kg and 3.06 kg, respectively and specific heat capacity (c) of the fluid of water, thermal oil and air are 4200 J/kg°C, 2027 J/kg°C and 1000 J/kg°C, respectively. The temperature T_2 and T_1 are the thermal sensor measurement. If 1 Joule is equivalent to 1 joule = 2.7778 x 10^{-4} Wh, the thermal power in Wh can be calculated as follows:

$$P_{out2} = \frac{Q\ x\ 2.777x10^{-4}}{t} \quad (4)$$

where t is the time measurement between 9 a.m and 2 p.m (5 hours).
Finally, the total efficiency for hybrid photovoltaic thermal is calculated by:

$$\eta_{tot} = \frac{P_{out1}+P_{out2}}{P_{in}} x100\% \quad (5)$$

Table III
Measurement results for water as the media of fluid

Time	V (V)	I (A)	T_1 (°C)	T_2 (°C)	ΔT (°C)	Q (Joule)	P_{out1} (W)	P_{out2} (W)	P_{in} (W)	$_{Total}$ (%)
Clear sky measurement, Monday 11 February 2013										
09.00	18.98	0.065	43	31	0	0	1.23	0	12.337	10
09.30	18.67	0.065	43	31	1	63000	1.21	0	12.135	10
10.00	18.57	0.065	44	31	2	126000	1.2	0	12.07	10
10.30	13.88	2.7	45	34	3	18900	37.48	10.5	374.76	12.801
11.00	14.08	2.8	46	36	5	315000	39.42	17.5	394.24	14.43
11.30	14.02	2.8	48	38	7	441000	39.26	24.5	392.56	16.24
12.00	14.2	2.8	49	38	7	441000	39.76	24.5	397.6	16.16
12.30	14.06	2.8	50	39	8	504000	39.37	28	393.68	17.11
13.00	14.06	2.8	50	40	9	567000	39.37	31.5	393.68	18
13.30	13.66	2.7	52	41	10	630000	36.88	35	368.82	19.48
14.00	13.97	2.7	52	44	13	819000	37.72	45.5	377.19	22.06
Cloudy sky measurement, Saturday 16 February 2013										
09.00	18.92	0.065	36	31	0	0	1.22	0	12.29	10
09.30	18.7	0.065	38	31	0	0	1.21	0	12.15	10
10.00	18.67	0.065	40	31	0	0	1.21	0	1213	10
10.30	18.45	0.065	41	31	0	0	1.19	0	11.99	10
11.00	18.68	0.065	44	31	0	0	1.21	0	12.14	10
11.30	12.01	2.5	46	33	2	126000	30.02	7	300.25	12.33
12.00	12.54	2.7	47	34	3	189000	33.85	10.5	338.58	13.10
12.30	12.47	2.7	48	34	3	189000	33.67	10.5	336.69	13.11
13.00	12.38	2.7	48	35	4	252000	33.42	14	334.26	14.18
13.30	12.11	2.6	47	36	5	315000	31.5	17.5	314.86	15.55
14.00	12.29	2.7	48	37	6	378000	33.18	21	331.83	16.32
Rainy measurement, Tuesday 19 February 2013										
09.00	18.2	0.065	32	31	0	0	1.18	0	11.83	10
09.30	18.37	0.065	32	31	0	0	1.19	0	11.94	10
10.00	18.15	0.065	32	31	0	0	1.17	0	11.79	10
10.30	17.89	0.065	32	31	0	0	1.16	0	11.62	10
11.00	18.57	0.065	33	31	0	0	1.2	0	12.07	10
11.30	18.53	0.065	36	31	0	0	1.2	0	12.04	10
12.00	18.63	0.065	38	31	0	0	1.21	0	12.10	10
12.30	18.72	0.065	41	31	0	0	1.21	0	12.16	10
13.00	18.81	0.065	44	31	0	0	1.22	0	12.22	10
13.30	11.76	2.5	45	33	2	126000	29.4	7	294	12.38
14.00	12.05	2.5	45	34	3	189000	30.12	10.5	301.25	13.48

TABLE IV
Measurement results for thermal oil as the media of fluid

Time	V (V)	I (A)	T_1 (°C)	T_2 (°C)	ΔT (°C)	Q (Joule)	P_{out1} (W)	P_{out2} (W)	P_{in} (W)	$_{Total}$ (%)
Clear sky measurement, Monday 25 March 2013										
09.00	18.89	0.065	42	31	0	0	1.22	0	12.27	10
09.30	18.77	0.065	43	31	0	0	1.22	0	12.20	10
10.00	11.23	1.2	45	34	3	10945.8	13.47	0.6	134.76	10.45
10.30	11.45	1.2	46	36	5	18243	13.74	1.01	137.4	10.73
11.00	11.67	1.2	48	38	7	25540.2	14.004	1.41	140.04	11.01
11.30	11.62	1.3	49	40	9	32837.4	15.1	1.82	151.06	11.20
12.00	11.54	1.3	50	40	9	32837.4	15.002	1.82	150.02	11.21
12.30	11.75	1.2	50	41	10	36486	14.1	2.02	141	11.43
13.00	11.6	1.3	51	43	12	43783.2	15.08	2.43	150.8	11.61
13.30	11.51	1.3	52	44	13	47431.8	14.96	2.63	149.63	11.76
14.00	11.63	1.3	51	45	14	51080.4	15.11	2.83	151.19	11.87
Cloudy sky measurement, Tuesday 9 April 2013										
09.00	18.72	0.065	39	31	0	0	0.121	0	1.21	10
09.30	18.67	0.065	40	31	0	0	0.121	0	1.21	10
10.00	18.58	0.065	42	31	0	0	0.12	0	1.20	10
10.30	18.53	0.065	43	31	0		0.12	0	1.20	10
11.00	18.62	1.2	44	31	0	0	22.34	0	223.44	10
11.30	11.78	1.3	45	32	1	3648.6	15.31	0.202	153.14	10.13
12.00	11.69	1.3	47	35	4	14594.4	15.19	0.81	151.97	10.53
12.30	11.72	1.2	48	36	5	18243	14.06	1.01	140.64	10.72
13.00	11.8	1.2	49	37	6	21891.6	14.16	1.21	141.6	10.85
13.30	11.76	1.2	50	39	8	29188.8	14.11	1.62	141.12	11.14
14.00	11.53	1.2	50	40	9	32837.4	13.83	1.82	138.36	11.31
Rainy measurement, Friday 8 March 2013										
09.00	18.67	0.065	39	31	0	0	1.21	0	12.13	10
09.30	18.43	0.065	43	31	0	0	1.19	0	11.97	10
10.00	9.73	1.2	45	36	5	18243	11.67	1.01	116.76	10.86
10.30	11.85	1.2	46	37	6	21891.6	14.22	1.21	142.2	10.85
11.00	18.87	0.065	43	35	4	14594.4	1.22	0.81	12.26	16.61
11.30	19.01	0.065	42	32	1	3648.6	1.23	0.2	12.35	11.64
12.00	18.97	0.065	43	32	1	3648.6	1.23	0.2	12.33	11.64
12.30	18.76	0.065	44	33	2	7297.2	1.21	0.4	12.19	13.32
13.00	18.64	0.065	44	32	1	3648.6	1.21	0.2	12.11	11.67
13.30	18.68	0.065	41	32	1	3648.6	1.21	0.2	12.14	11.66
14.00	18.8	0.065	41	31	0	0	1.22	0	12.22	10

Table III shows the testing results of controller performance using water as the media fluid. There are three different sky conditions for the measurement, i.e clear, cloudy and rainy. In the electrical output, current and voltage measurement are influenced by the operation of windshield whiser pump. During the pump operation, the load of control circuit becomes non-linear, while it is linear when the pump is off. Under clear sky measurement, the efficiency starts increasing to 12.801% at 10.30 a.m and continuing to 22.06% at the end of experimental works (2 p.m). It means that the much higher efficiency may be expected at the late of afternoon where the hot water is needed for households. Under cloudy sky operation, the increasing output is little late and also the final efficiency system is lower than that of clear sky operation result. The efficiency is getting worst under rainy operation where the intensity of sunlight is low. However, the control system is response fast once the rainy stops and the PV panel receiving sunlight at 1 p.m.

TABLE V
Measurement results for air as the media of fluid

Time	V (V)	I (A)	T_1 (°C)	T_2 (°C)	ΔT (°C)	Q (Joule)	P_{out1} (W)	P_{out2} (W)	P_{in} (W)	$_{Total}$ (%)
Clear sky measurement, Thursday 21 March 2013										
09.00	19.38	0.065	44	35	0	0	1.25	0	12.59	10
09.30	19.11	0.065	44	36	1	3060	1.24	0.17	12.42	11.36
10.00	18.47	0.065	45	38	3	9180	1.2	0.51	12	14.24
10.30	18.62	0.065	46	39	4	12240	1.21	0.68	12.103	15.61
11.00	18.68	0.065	48	40	5	15300	1.21	0.85	12.142	17
11.30	18.93	0.065	49	41	6	18360	1.22	1.02	12.30	18.28
12.00	18.87	0.065	51	40	5	15300	1.24	0.85	12.26	16.93
12.30	19.1	0.065	51	42	7	21420	1.23	1.19	12.41	19.58
13.00	18.95	0.065	52	43	8	24480	1.23	1.36	12.31	21.04
13.30	18.72	0.065	53	45	10	30600	1.21	1.7	12.16	23.97
14.00	18.56	0.065	53	46	11	33660	1.2	1.87	12.064	25.5
Cloudy sky measurement, Saturday 23 March 2013										
09.00	19.51	0.065	42	33	0	0	1.26	0	12.68	10
09.30	19.3	0.065	43	33	0	0	1.25	0	12.54	10
10.00	18.93	0.065	44	35	2	6120	1.23	0.34	12.30	12.76
10.30	18.72	0.065	46	36	3	9180	1.21	0.51	12.16	14.19
11.00	18.81	0.065	47	38	5	15300	1.22	0.85	12.22	16.95
11.30	19.05	0.065	48	39	6	18360	1.23	1.02	12.38	18.23
12.00	18.96	0.065	49	40	7	21420	1.23	1.19	12.32	19.65
12.30	18.75	0.065	50	40	7	21420	1.21	1.19	12.18	19.76
13.00	18.77	0.065	50	41	8	24480	1.22	1.36	12.20	21.14
13.30	18.82	0.065	51	42	9	27540	1.22	1.53	12.23	22.50
14.00	18.5	0.065	52	43	10	30600	1.20	1.7	12.02	24.13
Rainy measurement, Thursday 7 March 2013										
09.00	17.8	-	-	-	-	-	-	-	-	-
09.30	17.9	-	-	-	-	-	-	-	-	-
10.00	17.4	-	-	-	-	-	-	-	-	-
10.30	19.4	0.065	36	34	0	0	1.25	0	12.58	10
11.00	18.6	0.065	44	37	3	9180	1.2	0.51	12.09	14.21
11.30	18.1	0.065	40	36	2	6120	1.17	0.34	11.77	12.88
12.00	18.4	0.065	42	36	2	6120	1.19	0.34	11.97	12.83
12.30	18.7	0.065	45	38	4	12240	1.21	0.68	12.16	15.58
13.00	18.6	0.065	45	37	3	9180	1.2	0.51	12.09	14.21
13.30	18.4	0.065	46	38	4	12240	1.19	0.68	11.94	15.69
14.00	18.5	0.065	48	40	6	18360	1.2	1.02	12.00	18.49

By comparing the efficiency in previous measurement where water as the media fluid, the lower efficiency is found in thermal oil as the media fluid. The measurement results are shown in Table IV under clear, cloudy and rainy operation. It is due to the lower specific heat capacity of thermal oil compared to the water. However, the thermal oil has higher viscosity that makes the pump needs extra works to flow the thermal oil from the storage fluid to the box extraction; means consuming much power from the PV module output that is consequently reducing the efficiency. The average efficiency for the system operation using thermal oil is about 11.87%. In fact, the high viscosity giving advantage to keep the stable efficiency, even though the weather condition is dramatically changing during day operation.

The testing our proposed control design using air as the media fluid is quite unique. The performance of windshield whiser pump is not so hard by comparing when the motor pumps the water and oil from the fluid storage to the heat box extraction. Consequently, the electrical power consumed by the motor is not so high that makes the efficiency is higher than the two previous measurements. During clear sky and cloudy, the overall performance can reach 25% and even 18% under rainy condition at the end of measurement. The measurement

result is shown in Table V. For all measurements, the performance and efficiency system are highly affected from the pump operation since the input power for the motor is taken from the PV module output.

Our proposed control system for hybrid photovoltaic thermal is designed for small scale PV system. However, it is also suitable for high capacity installation of PV system. To do so, it is important to modify the hardware and software of the current design system. The hardware components that need to be modify is heat box extraction, dimension of pipe and fluid storage. For instance, with 10 PV modules in series, the dimension of heat box extraction will be 850x55x10 cm^3, consequently affecting the dimension of pipe and increasing the fluid volume in fluid storage. In terms of software modification, it is highly depending on the type of motor pump. The utilization of AC motor is possible, however additional inverter system must be added since the powering of motor is coming from PV module output; therefore the wiring system is getting much more complex.

Improving control system for the hybrid photovoltaic thermal is one of the ways to enhance the performance of system and to increase the efficiency. Our experimental design is very simple therefore the efficiency is not so high but it still may open to be increased. The part that is important to be improved is the material and thermal insulation of the heat box extraction. Instead of using wood and plastic for the box extraction, the Aluminum, galvanized steel plate with using polyurethane and fibre-glass wool can be recommended to keep the heat much longer in time. Adding heat storage components will be also very useful for the thermal utilization at night. If our proposed design system comes up with very sophisticated components and materials, the expected efficiency may reach above 60%. However, getting complex technical system will be consequent to increase the overall cost of the system.

V. Conclusion

The paper has explained the control mechanism in hybrid photovoltaic thermal using microcontroller ATmega8535. Two thermal sensors are utilized in this experimental works. The first thermal sensor of LM35D2 is located inside the thermal box extraction to measure the temperature at back side of PV module as the heat source. Another thermal sensor of LM35D2 is located inside the fluid storage to measure the fluid outlet temperature. If the temperature inside the box extraction reaches value higher than 45°C then microcontroller operates windshield whiser motor to pump the fluid through the spiraling pipe back to the fluid storage. The control process stops once the temperatures between two thermal sensors are equal. Several testing on three different fluids, air, water and thermal oil under clear sky, cloudy sky and rainy condition are conducted in order to confirm the proper working condition of controller. The advantage of this system is the simple algorithm with high potential of efficiency improvement by implementing sophisticated materials and components and may be useful for high capacity of PV installation.

Acknowledgment

We would like to acknowledge Ms. Nur Hasfiana H for the great contribution in real-time experiment and positive efforts in data measurement.

References

[1] Chow, ‘A review on photovoltaic/thermal hybrid solar technology’, Applied Energy, Vol. 87, No.2, pp. 365-379, 2010
[2] Nagano, et.al, ‘Development of thermal-photovoltaic hybrid exterior wallboards incorporating PV cells in and their winter performances’, Solar Energy Materials and Solar Cells, Vol. 77, No. 3, pp. 265-282, 2003
[3] Anand & Tiwari, ‘Energy and exergy efficiencies of a hybrid photovoltaic–thermal (PV/T) air collector‘, Renewable Energy, Vol. 32, No. 13, pp. 2223-2241, 2007
[4] Agarwal & Tiwari, ‘Energy and exergy analysis of hybrid micro-channel photovoltaic thermal module’, Solar Energy, Vol. 85, No. 2, pp. 356-370, 2011
[5] Jie, et.al, ‘Effect of fluid flow and packing factor on energy performance of a wall-mounted hybrid photovoltaic/water-heating collector system’, Energy and Buildings, Vol. 38, No. 12, pp. 1380-1387, 2006
[6] Jie, et.al, ‘A sensitivity study of a hybrid photovoltaic/thermal water-heating system with natural circulation’, Applied Energy, Vol. 84, No. 2, pp. 222-237, 2007
[7] da Silva & Fernandez, ‘Hybrid photovoltaic/thermal (PV/T) solar systems simulation with Simulink/Matlab’, Solar Energy, Vol. 84, No. 12, pp. 1985-1996, 2010
[8] Vokas, et.al, ‘Hybrid photovoltaic–thermal systems for domestic heating and cooling - A theoretical approach’, Solar Energy, Vol. 80, No. 5, pp. 607-615, 2006
[9] Pearce, ‘Expanding photovoltaic penetration with residential distributed generation from hybrid solar photovoltaic and combined heat and power systems’, Energy, Vol. 34, No. 11, pp. 1947-1954, 2009
[10] Pathak et.al, ‘The effect of hybrid photovoltaic thermal device operating conditions on intrinsic layer thickness optimization of hydrogenated amorphous silicon solar cells’, Solar Energy, Vol. 86, No. 9, pp. 2673-2677, 2012
[11] Pathak, ‘Effects on amorphous silicon photovoltaic performance from high-temperature annealing pulses in photovoltaic thermal hybrid devices’, Solar Energy Materials and Solar Cells, Vol. 100, pp. 199-203, 2012
[12] Mishra & Tiwari, ‘Energy matrices analyses of hybrid photovoltaic thermal (HPVT) water collector with different PV technology’, Solar Energy, Vol. 91, pp. 161-173, 2013